Int J Clin Exp Pathol 2017;10(11):11114-11121
www.ijcep.com /ISSN:1936-2625/IJCEP0058665

Original Article

Expression of Tiam1 and Rac1 proteins in renal cell carcinoma and its clinical-pathological features

Guang Shan[1], Tian Tang[2], Huijun Qian[1], Yue Xia[1]

Departments of [1]Urologic II, [2]Oncology II, Renmin Hospital of Wuhan University, Wuhan, Hubei, China

Received June 2, 2017; Accepted August 9, 2017; Epub November 1, 2017; Published November 15, 2017

Abstract: Purpose: To explore the connections between Tiam1 and Rac1 expression in renal cell carcinoma (RCC), and its pathological type, grading, invasion and metastasis. Methods: Tiam1 and Rac1 expression was measured in 60 specimens of RCC (including 42 clear cell cases, 12 papillary cases, and 6 chromophobe cases) and a 10-specimen control group using quantum dots IHC labeling, complete with clinical and pathological records, dated 2008 to 2014, were taken from the archives of the Department of Pathology, People's Hospital of Wuhan University. The expressions of Tiam1 and Rac1 proteins in specimens were measured using immunohistochemical (IHC) and quantum dots-labeling methods to examine their relationships to the clinical and pathological characteristics of RCC. The HIPAS-1000 software was used to quantitatively analyze on the results to obtain absorbance and positive area ratio (PAR) values, and SPSS 15.0 was used to perform single-factor analysis of variance and q verification. Spearman's rank correlation test is used to verify the correlation between absorbance and PAR of the two proteins. Results: 1. QDs IHC staining. Tiam1 and Rac1 expression is high in RCC, and low in surrounding tissues ($P<0.05$). 2. Expression levels of both proteins show no correlation with patient sex, age, or tumor size ($P>0.05$), yet correlate with the differentiation, stage, and lymphatic metastasis of tumors ($P<0.05$). Spearman's test shows a positive correlation between the expression levels of Tiam1 and Rac1 in RCC tissues ($r=0.425$, $P<0.05$). Conclusion: 1. Abnormal Tiam1 and Rac1 expression may be an early molecular event in RCC, suggesting they are carcinogens related to proto-oncogenes. 2. Tiam1 and Rac1 expression levels correlate with the differentiation, stage, and lymphatic metastasis of RCC, suggesting they play important roles in its invasion and metastasis. 3. The expression levels of Tiam1 and Rac1 are positively correlated within RCC, suggesting a synergy between the two in controlling its pathogenesis and development.

Keywords: Renal cell carcinoma, Tiam1, Rac1, pathological feature, quantum dots, immunohistochemistry

Introduction

Renal cell carcinoma (RCC) is one of the most common malignant tumors of the urinary system. Originating from the endothelial systems of uriniferous tubules in the renal parenchyma, it accounts for 80~90% of malignant tumors in kidneys [1], and has a still-rising occurrence rate only second to bladder cancer among tumors of the urinary system, The mechanism behind RCC's genesis is still poorly understood; since immune-, chemo-, and radiation therapies have not been effective, surgery remains the most important approach to its treatment. However, middle-to-late stage RCC has shown high rates of postoperative recurrence and distant metastasis [2]. Due to its insensitivity to radio- and chemotherapy, research on RCC has focused on early diagnosis, timely and appropriate intervention, suppression of invasion and metastasis, and raising survival rates.

Tiam1 was first discovered by Habets et al. (1994) during in vitro selection of invasive T-lymphoma cells [3]. They named it "T-cell lymphoma invasion and metastasis-inducing protein 1" (TIAM1) due to its ability to enhance invasiveness in T-lymphoma cells. It is a specific guanine nucleotide exchange factor (GEF) for Ras-related C3 botulinum toxin substrate 1 (RAC1), a member of the Rho family of small G proteins. When stimulated by extracellular signals, Tiam1 can promote Rac1 to transform from an inactive GDP-bound state to an active

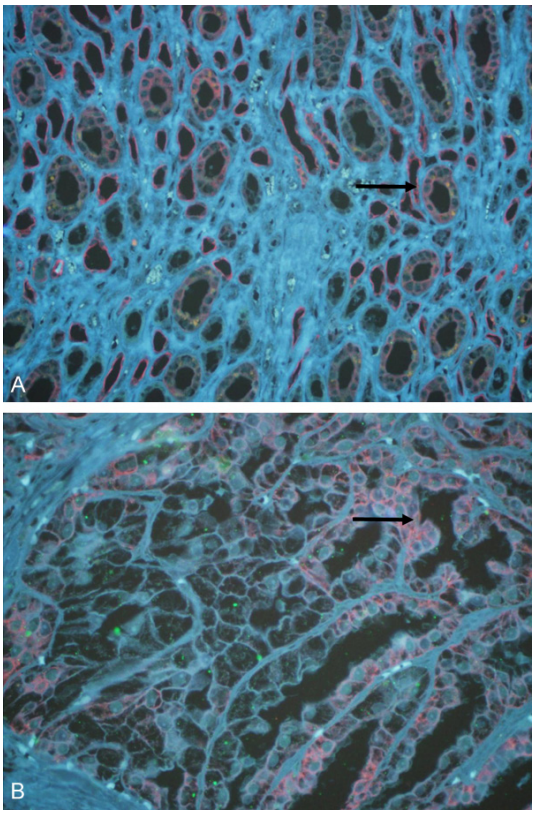

Figure 1. Expression of detecting Tiam1 and Rac1 in renal cell carcinoma tissues by using Quantum-dots staining. A: Tiam1 expression in renal cell carcinoma tissues. Positive Tiam1 expression was mainly discovered in cell plasm or cell membrane. The plasm or cell membrane of renal cell carcinoma tissues cells exhibited a strong red fluorescence, indicating a high expression of Tiam1 (black arrow); B: Rac1 expression in renal cell carcinoma tissues. Positive Rac1 expression was mainly discovered in cell plasm or cell membrane. The plasm or cell membrane of renal cell carcinoma tissues cells exhibited a strong red fluorescence, indicating a high expression of Rac1 (black arrow).

GTP-bound state [4, 5]. The activated Rac1-GTP can interact with various downstream effector molecules to influence events related to invasion and metastasis, including reconstruction of cellular skeletons, cell-cell adhesion, expression and regulation of genes, cellular movements, and cellular apoptosis [6].

This study sets out to measure the expression levels of Tiam1 and Rac1 in RCC and surrounding tissues using quantum dots (QDs) and IHC technologies, analyze the relationships between their expressions and the clinical and pathological features of RCC, and present a preliminary analysis of their relationship to each other and roles in its genesis, development, invasion and metastasis, in hope of providing new evidences to clinical exploration into the biological behavior of RCC, and lay the theoretical basis for its targeted therapy.

Materials and methods

Materials

60 paraffin-embedded specimens of RCC (comprising 42 clear cell cases, 12 papillary cases, and 6 chromophobe cases), and 10 specimens of surrounding kidney tissues, dated 2008 to 2014, complete with clinical and pathological records, were taken from the archives of the Department of Pathology, People's Hospital of Wuhan University. Of the specimens, 36 cases were males, and 24 were females, with patient age ranging from 28 to 86, for an average of 56.63 years. All specimens were first occurrences, without any chemo- or other therapies before surgery, and pathologically diagnosed to be RCC post-surgery. Clinical Robson staging divided them into 13 in Stage I, 24 in Stage II, 12 in Stage III, and 11 in Stage IV, and histopathological staging graded them into 14 in G1, 27 in G2, and 19 in G3. 15 specimens of kidney tissues 2.5 cm away from tumors were selected as the normal control group.

Thoenes' system of pathology grading

G1 (well-differentiated): normal-sized round nuclei; delicate or condensed chromatins; generally one normal-sized nucleolus in or slightly off the center of each nucleus; no mitotic figure.

G2 (differentiated): intermediately enlarged round or oval nuclei, frequently with ruffles; delicate, coarse, or dense chromatins; a saliently enlarged nucleolus in or slightly off the center of each nucleus; some mitotic figures.

G3 (low- or undifferentiated): saliently enlarged nuclei, often irregular in shape; thick and irregular chromatins; one or more nucleoli in each nucleus; frequent pathological mitotic figures.

Main reagents

1. Instant-use rabbit anti-human polyclonal antibodies for Tiam1 and Rac1; 2. Instant hypersensitive streptavidin-peroxidase (SP) IHC kit; 3. DAB coloration kit and poly-lysine; 4. QDs hypersensitive fluorescent reagent kit, provided by Wuhan Jiayuan Quantum Dots Co, Ltd.

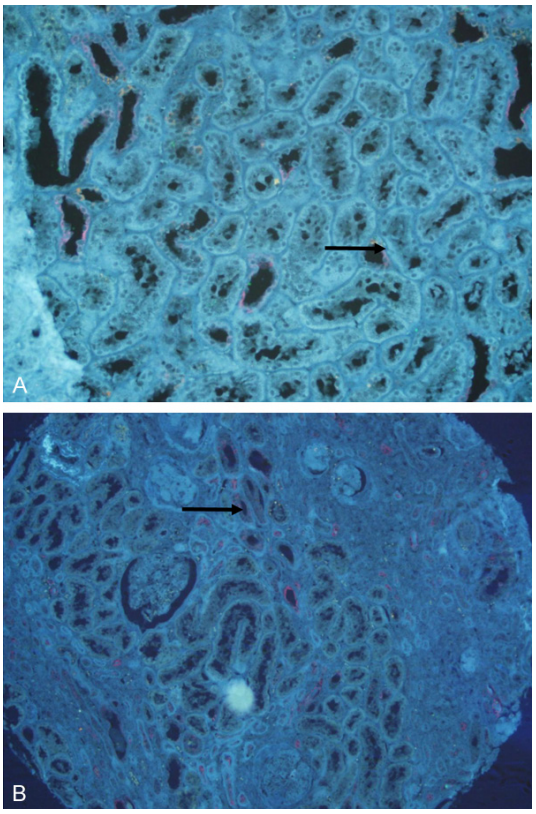

Figure 2. Expression of detecting Tiam1 and Rac1 in cancer side tissue by using Quantum-dots staining. A: Tiam1 expression in cancer side tissue. Positive Tiam1 expression was mainly in cell plasm or cell membrane. The plasm or cell membrane of cancer side tissue exhibited a weak or no red fluorescence, Tiam1 was lowly expressed in cancer side tissue (black arrow). B: Rac1 expression in cancer side tissue. Positive Rac1 expression was mainly in cell plasm or cell membrane. The plasm or cell membrane of cancer side tissue exhibited a weak or no red fluorescence, Tiam1 was lowly expressed in cancer side tissue (black arrow).

Measuring Tiam1 and Rac1 expression with QDs-SA

RCC tissue sections (thickness, 4 μm) were dewaxed and hydrated, and underwent microwave antigen retrieval; sections were swashed with TBS, sealed with buffer solution, and incubated in wet chamber at 37°C for 30 min; sections were dripped with Tiam1 and Rac1 antibodies, and incubated at 37°C for 2 h; sections were swashed with TBS-T for 3×3 min, sealed with buffer solution, and incubate in wet chamber at 37°C for 10 min; sections were dripped with biotin goat anti-mouse IgG, and incubated in wet chamber at 37°C for 30 min; sections were swashed with TBS-T for 3×3 min, sealed with buffer solution, and incubated in wet chamber at 37°C for 10 min; sections were dripped with QDs-SA diluted with buffer solution (1: 100), and incubated in wet chamber at 37°C for 30~60 min; sections were swashed with TBS-T for 3×3 min, dripped with 50% glycerin, and packed into microarrays; a fluorescence microscope was used to observe the arrays, and incite Qd602 with various wavelengths. Positive signals from Tiam1 and Rac1 were observed. The appearance of orange-red fluorescent particles is considered positive; protein expression is considered positive when the positive area ratio is equal to or above 25%. A negative control group was similarly prepared, with TBS buffer solution replacing the primary antibodies.

The entire test process does not require protection from light.

Result determination

For QDs-SA staining, the reaction was considered positive when a significant amount of red fluorescence was observed in the cell membrane or cytoplasm. No such reaction is supposed to occur in the negative control group.

The HPIAS-1000 high-resolution image analysis and reporting system developed by Tongji Qianping Imaging Engineering Co. was used to perform the quantitative analysis. From each section, five random, intact and non-overlapping views were taken at ×400 magnification. For each view, measurements were made for the total area of cells, to compute the mean absorbance, the total area of regions with positive reactions, and the final positive area ratio (PAR). The averages of mean absorbance and PAR from five views in each section were used as its results. (PAR = total area of positive reactions in unit area/total area of cells in unit area ×100%).

Statistical methods

The SPSS 15.0 software is used for statistical analysis, which include single-factor analysis and q verification on the mean absorbance and PAR values, with $\alpha=0.05$. Spearman's rank correlation is used to analyze correlations between results, with $P<0.05$ indicating statistical significance.

Table 1. Mean optical density (MOD) and positive area ratio (PAR) for Tiam1 proteins expressions in Renal cell carcinoma and cancer side tissue ($\bar{x}\pm s$)

Group	No. of cases	Average optical density	Positive rate of area
RCC	60	0.2839±0.0075*	0.2978±0.0077*
Cancer side tissue	10	0. 0874±0.0030	0.0790±0.0029

*RCC vs. cancer side tissue, $P<0.05$.

Table 2. Mean optical density (MOD) and positive area ratio (PAR) for Rac1 proteins expressions in Renal cell carcinoma and cancer side tissue ($\bar{x}\pm s$)

Group	No. of cases	Average optical density	Positive rate of area
RCC	60	0.3005±0.0078*	0.2990±0.0078*
Cancer side tissue	10	0.0867±0.0031	0.0787±0.0028

*RCC vs. cancer side tissue, $P<0.05$.

Results

QDs-SA staining

Under the excitation of UV, blue and green lights from the fluorescence microscope, certain areas in the QDs-marked RCC and surrounding tissues could be clearly seen to emit red-orange lights, indicating the presence of Tiam1 and Rac1. The clean backgrounds suggest absence of any nonspecific binding. The areas of positive Tiam1 and Rac1 expression were located in the cytoplasm or cell membranes. The red fluorescence was particularly strong in the cytoplasm and cell membranes of cancerous tissues, pointing to high expression of target proteins (**Figure 1A** and **1B**); Very small amounts of such fluorescence can be seen in the cytoplasm and cell membranes of surrounding tissues, indicating weak or nonexistent expression (**Figure 2A** and **2B**). **Table 1** shows the results of analysis. The q test indicates significant differences ($P<0.05$) between cancerous and surrounding tissues in mean absorbance and PAR (**Tables 1**, **2**).

Correlations between Tiam1/Rac1 protein expressions and pathological type, tumor size, sexes, age groups of RCC

The expression levels of Tiam1 and Rac1 have been shown to be related to differentiation, clinical staging and lymphatic metastasis ($P<0.05$) (**Tables 3**, **4**), but unrelated to patient tumor sizes, age and sex ($P>0.05$) (**Table 5**).

Correlations between Tiam1 and Rac1 expressions in RCC tissues

Spearman's rank correlation analysis shows the expressions of Tiam1 and Rac1 are positively correlated ($r=0.425$, $P<0.05$).

Discussion

RCC refers to a category of tumors occurring in endothelial cells of uriniferous tubules. It is the most common malignant tumor in the urinary system of adults, with an occurrence rate only second to bladder cancer among tumors of the urinary system, accounting for 90% of malignant tumors in kidneys in adults, and 2~3% of all human malignant tumors [7]. Often seen in males aged 50 to 60, its causes are not fully understood, and may be related to smoking [8], obesity [9], prolonged hemodialysis, high blood pressures, and antihypertension treatments [10]. The 2004 WHO standard of pathological classification divides RCC into the clear cell, papillary, chromophobe, and unclassified varieties. Clear cell RCC is the most common, accounting for 70~80% of all occurrences [11, 12]. RCC occurrences display significant regional variations, with remarkably higher occurrences in developed compared to developing countries [13]. In China, urban regions have significantly higher RCC occurrences than rural regions, which can be as high as 43 times that of the latter. RCC tissues first appear as local growths in the renal parenchyma, and upon reaching certain sizes may compress surrounding tissues and damage the renal pelvis and calyces. With further development, the tumor may invade and penetrate the renal capsule, causing invasion of blood vessels or lymph nodes, or further metastasis to other organs. The complex behavior and characteristics of RCC, including mechanisms of its genesis, development, invasion and metastasis are not fully understood. Clinically, predictions on its progression, recurrence and prognosis largely depend on its clinical staging and pathological grading.

The invasion and metastasis of malignant tumors are results of complex multistage interac-

Table 3. Correlations between Tiam1/Rac1 protein expressions and Clinical stage and the differentiation degree of RCC

Stage	Cases	Tiam1			Rac1		
		Pos	Neg	Pos.%	Pos	Neg.	Pos.%
I	13	6	7	46.1%	5	8	38.5%
II	24	19	5	79.1%	18	6	75.0%
III	12	10	2	83.3%	11	1	91.6%
IV	11	11	0	100.0%*	11	0	100.0%*
Degree of Differentiation							
High	14	5	9	35.7%	6	8	42.8%
Medium/Low	46	27	19	58.6%*	28	18	60.8%*

*Fisher exact probability tests return $P<0.05$, indicating the results are significant.

Table 4. Correlations between Tiam1/Rac1 protein expressions and lymphatic metastasis of RCC

Lymph node metastasis	Cases	Tiam1			Rac1		
		Pos.	Neg.	Pos.%	Pos.	Neg.	Pos.%
Yes	18	16	2	88.8%	17	1	94.5%
No	42	18	24	42.8%*	17	25	40.4%*

*Fisher exact probability tests return $P<0.05$, indicating the results are significant.

Table 5. Correlations between Tiam1/Rac1 protein expressions, tumor sizes, age and sexes

Pathological features	Cases	Tiam1			Rac1		
		Pos.	Neg.	Pos.%	Pos.	Neg.	Pos.%
Tumor size (cm)							
≥4	38	28	10	73.6%	26	12	68.4%
<4	22	14	8	63.6*	13	9	59.0%*
Age							
≥65	33	22	11	66.7%	23	10	69.6%
<65	27	16	11	59.1*	17	10	62.9%*
Sex							
Male	36	23	13	63.8%	22	14	61.1%
Female	24	14	10	58.3*	14	10	58.3%*

*Fisher exact probability tests return $P>0.05$, indicating the results are no significant.

tions between tumor cells, host stroma, and host cells, involving many genes and their products. A tumor cell's capacity for invasion and metastasis is strongly connected to its capacity for movement [14] involving processes including cell adhesion, cell movement, proliferation, degradation of extracellular matrix, genesis of tumor vessels, and host immunity. Skeletal structures determine the different movement capacities of cells, which are one area where normal cells differ from tumor cells of varying metastasis potentials [15]. In addition to maintaining the shape and movement of cells, skeletons also serve to transmit extra- and intracellular signals, and participate in cellular activities such as secretion, contact inhibition, proliferation and apoptosis. Since a specific marker has yet to be found that can simplify its early diagnosis, RCC patients are often not discovered until later stages [16]. As conventional histopathological analysis proves ineffective, a molecular biological approach may be more helpful in understanding the mechanism, choice of treatment and prognosis of RCC.

The T-cell lymphoma invasion and metastasis-inducing protein 1, or Tiam1 was found by Habets et al. during in vitro selection of invasive T-lymphoma cells. It partakes in processes like reconstruction of cell skeletons, cellular polarization, cell movement and migration, gene expressions, proliferation and apoptosis [17-19]. The expression of Tiam1 is strongly connected to the genesis and development of tumors. As a specific GEF for Rac1, it regulates biological processes by causing the latter to transform from the inactive Rac1-GDP to Rac1-GTP [20, 21]. The influence of the Tiam1-Rac1 signal on cells is cell-specific and matrix-specific. When a cell's substrates consist of fibronectin and laminins, the cell displays stronger inter-cellular adhesion, and Tiam1 is localized in areas of adhesive contact between cells, where adhesive complexes such as E-cadherin are also localized. When the substrates consist of Type I collagen, the cell displays better movement capacity, and Tiam1 is localized in its membrane ruffles and cytoplasm. Therefore the substrates can directly or indirectly regulate the activities of Rac1 via Tiam1, and determine whether a cell is adhesive or mobile. On the

other hand, the alternation between adhesion and migratory movement is essential to the invasion and metastasis of tumor cells; it is therefore likely that Tiam1-Rac1 regulation plays a part in these processes [22].

In 1998, Alivisatos and Nie reported on the same issue of Science about their foundational work in using QDs for biological marking and cell imaging, presenting the earliest solutions to the target-specificity and biocompatibility of QDs as a biological probe [23]. QDs have shown great potential in biomedical analysis due to possessing properties that far surpass conventional fluorescent labelers [24, 25]. By binding to large molecules, QDs can label different parts or components of cells with different colors, and enable nonspecific detection and quantitative analysis of proteins through fluorescence resonance energy transfer.

Many conventional biomedical methods face limitations in applications demanded by the advancement of imaging technologies, such as direct real-time analysis of interactions between biological molecules. QDs have very good photophysical properties including: 1) wide excitation spectra that can be continuously adjusted; 2) large Stokes displacements, low spectral overlap, and high sensitivity; 3) strong resistance to photobleaching and longevity; 4) high photostability. They are also highly biocompatible, with no effect on normal physiological cellular activities including growth, development, migration and signal transmission [26, 27]. These advantages mean that QDs can be widely adopted for biomedical purposes including cellular, molecular and in vivo imaging in areas such as multicolor imaging of cellular structures, tracing of cell migration and differentiation, and imaging of labeled cells or lymph node and vessel systems [28]. They have particularly good prospects as an ideal marker in the study of tumors after certain modifications. Advancement of imaging technologies and QDs marking have enabled the real-time monitoring of biological activities on a molecular level, and brought new innovations to bioluminescent labeling, histological imaging, particle-based tracing, in vivo molecular positioning in animal and plant bodies, genomics and biochip development [29, 30].

In this study, we utilized a QDs IHC approach to measure Tiam1 and Rac1 expression in RCC tissues to examine their relationships to its genesis and development. The results show that both proteins have significantly higher expression levels in RCC than noncancerous renal tissues, and may be closely connected to the cancer's development. We speculate that Tiam1 can activate Rac1 by stimulating the release of GDP and the binding with GTP, and the signal is transmitted by kinases to activate downstream molecules, thus performing functions including regulating skeletal reconstruction and cellular polarization, encouraging movement and migration, and participating in proliferation and apoptosis.

The expression levels of Tiam1 and Rac1 have been shown to be unrelated to patient sex, age and tumor size ($P>0.05$), but related to differentiation, clinical staging and lymphatic metastasis ($P<0.05$). This indicates their expression levels can be correlated to the clinical stages of RCC, being higher in later stages, and correlated to lymphatic metastasis processes. The study also shows that the two proteins have positively correlated expression levels, suggesting they are directly related in their functions in RCC, and the Tiam1-Rac1 signal route may play a part in the invasion and metastasis of RCC through the regulation of molecules related to cellular adhesion. The detection of the two proteins can also be used in the diagnosis of RCC and determining methods of treatment.

The formation of a tumor is due to a combination of multiple genes, processes and other factors. As we continue to explore the mechanism behind the lymphatic metastasis of RCC, it is hoped the study may serve to improve the determination, prediction and intervention of lymphatic metastasis in RCC patients.

Acknowledgements

This study was supported by a grant-in-aid (81402242) from the National Natural Science Foundation of China (youth fund).

Disclosure of conflict of interest

None.

Address correspondence to: Guang Shan, Department of Urologic II, Renmin Hospital of Wuhan University, Wuhan 430060, Hubei, China. Tel: +86-27-88041919-87629; E-mail: 13871008306@163.com

References

[1] Wallin U, Rothenberger D, Lowry A, Luepker R, Mellgren A. CEA-a predictor for pathologic complete response after neoadjuvant therapy for rectal cancer. Dis Colon Rectum 2013; 7: 859-868.

[2] Bhatt JR, Jewett MA, Richard PO, Kawaguchi S, Timilshina N, Evans A, Alibhai S, Finelli A. Multilocular cystic renal cell carcinoma: pathological T staging makes no difference to favorable outcomes and should be reclassified. J Urol 2016; 196: 1350-1355.

[3] Habets GG, Scholtes EH, Zuydgeest D, van der Kammen RA, Stam JC, Berns A, Collard JG. Identification of an invasion-inducing gene, Tiam-1, that encodes a protein with homology to GDP-GTP exchangers for Rho-like proteins. Cell 1994; 77: 537-549.

[4] Niebel B, Wosnitza CI, Famulok M. RNA-aptamers that modulate the RhoGEF activity of Tiam1. Bioorg Med Chem 2013; 21: 6239-6246.

[5] Shepherd TR, Hard RL, Murray AM, Pei D, Fuentes EJ. Distinct ligand specificity of the Tiam1 and Tiam2 PDZ domains. Biochemistry 2011; 50: 1296-1308.

[6] Lane J, Martin TA, Mansel RE, Jiang WG. The expression and prognostic value of the guanine nucleotide exchange factors (GEFs) Trio, Vav1 and TIAM-1 in human breast cancer. Int Semin Surg Oncol 2008; 16: 23.

[7] Lindblad P. Epidemiology of renal cell carcinoma. Scand J Surg 2004; 93: 88-96.

[8] Bergström A, Hsieh CC, Lindblad P, Lu CM, Cook NR, Wolk A. Obesity and renal cell cancer-a quantitative review. Br J Cancer 2001; 85: 984-990.

[9] Pischon T, Lahmann PH, Boeing H, Friedenreich C, Norat T, Tjønneland A, Halkjaer J, Overvad K, Clavel-Chapelon F, Boutron-Ruault MC, Guernec G, Bergmann MM, Linseisen J, Becker N, Trichopoulou A, Trichopoulos D, Sieri S, Palli D, Tumino R, Vineis P, Panico S, Peeters PH, Bueno-de-Mesquita HB, Boshuizen HC, Van Guelpen B, Palmqvist R, Berglund G, Gonzalez CA, Dorronsoro M, Barricarte A, Navarro C, Martinez C, Quirós JR, Roddam A, Allen N, Bingham S, Khaw KT, Ferrari P, Kaaks R, Slimani N, Riboli E. Body size and risk of renal cell carcinoma in the European prospective investigation into cancer and nutrition (EPIC). Int J Cancer 2006; 118: 728-738.

[10] Walter M, Wetterauer C, Bruder E, Obermann EC, Subotic S, Wyler S. Renal cell carcinoma in a young adult - do we need further investigations? Urol Case Rep 2016; 6: 27-29.

[11] Lopez-Beltran A, Scarpelli M, Montironi R, Kirkali Z. 2004 WHO classification of the renal tumors of the adults. Eur Urol 2006; 49: 798-805.

[12] Lindblad P. Epidemiology of renal cell carcinoma. Scand J Surg 2004; 93: 88-96.

[13] Kuroda N, Yorita K, Nagasaki M, Harada Y, Ohe C, Jeruc J, Raspollini MR, Michal M, Hes O, Amin MB. Review of succinate dehydrogenase-deficient renal cell carcinoma with focus on clinical and pathobiological aspects. Pol J Pathol 2016; 67: 3-7.

[14] Seo AN, Yoon G, Ro JY. Clinicopathologic and molecular pathology of collecting duct carcinoma and related renal cell carcinomas. Adv Anat Pathol 2017; 24: 65-77.

[15] Afriansyah A, Hamid AR, Mochtar CA, Umbas R. Targeted therapy for metastatic renal cell carcinoma. Acta Med Indones 2016; 48: 335-347.

[16] Tornberg SV, Nisen H, Visapää H, Kilpeläinen TP, Järvinen R, Mirtti T, Kantonen I, Simpanen J, Bono P, Taari K, Järvinen P. Outcome of surgery for patients with renal cell carcinoma and tumour thrombus in the era of modern targeted therapy. Scand J Urol 2016; 50: 380-386.

[17] Zhu JM, Yu PW. Effects of Tiam 1 on invasive capacity of gastric cancer cells in vitro and underlying mechanisms. Asian Pac J Cancer Prev 2013; 14: 201-208.

[18] Demarco RS, Struckhoff EC, Lundquist EA. The Rac GTP exchange factor TIAM-1 acts with CDC-42 and the guidance receptor UNC-40/DCC in neuronal protrusion and axon guidance. PLoS Genet 2012; 8: e1002665.

[19] Vettel C, Wittig K, Vogt A, Wuertz CM, El-Armouche A, Lutz S, Wieland T. A novel player in cellular hypertrophy: Giβγ/PI3K-dependent activation of the RacGEF TIAM-1 is required for α_1-adrenoceptor induced hypertrophy in neonatal rat cardiomyocytes. J Mol Cell Cardiol 2012; 53: 165-175.

[20] Boehm M, Krause-Gruszczynska M, Rohde M, Tegtmeyer N, Takahashi S, Oyarzabal OA, Backert S. Major host factors involved in epithelial cell invasion of campylobacter jejuni: role of fibronectin, integrin beta1, FAK, Tiam-1, and DOCK180 in activating Rho GTPase Rac1. Front Cell Infect Microbiol 2011; 1: 17.

[21] Zhu JM, Yu PW. Downregulation of T-cell lymphoma invasion and metastasis-inducing factor 1 induces cytoskeletal rearrangement and inhibits the invasive capacity of gastric cancer cells. Mol Med Rep 2013; 8: 425-433.

[22] Zheng C, Diaz-Cuadros M, Chalfie M. GEFs and Rac GTPases control directional specificity of neurite extension along the anterior-posterior axis. Proc Natl Acad Sci U S A 2016; 113: 6973-6978.

[23] Bruchez M Jr, Moronne M, Gin P, Weiss S, Alivisatos AP. Semiconductor nanocrystals as fluorescent biological labels. Science 1998; 281: 2013-2016.

[24] Sharon E, Freeman R, Willner I. CdSe/ZnS qu an tum dot s-g-quad-ruplex/heminhyb rids as optical DNA sensors and aptasensors. Anal Chem 2010; 82: 7073-7.
[25] Yu G, Liang J. Synthesis and application of quantum dots FRET-based protease sensors. Chemist Biology 2006; 13: 723-731.
[26] Zheng J, Ghazani AA, Song Q, Chan WC and Wang C. Cellular imaging and surface marker labeling of hematopoietic cells using quantum dot bioconjugates. Lab Hematol 2006; 12: 94-98.
[27] Garon EB, Marcu L, Luong Q, Tcherniantchouk O, Crooks GM and Koeffler HP. Quantum dot labeling and tracking of human leukemic, bone marrow and cord blood cells. Leuk Res 2007; 31: 643-651.
[28] Mason JN, Tomlinson ID, Rosenthal SJ and Blakely RD. Labeling cell surface proteins via antibody quantum dot streptavidin conjugates. Methods Mol Biol 2005; 303: 35-50.
[29] Qu YG, Zhang Q, Pan Q, Zhao XD, Huang YH, Chen FC and Chen HL. Quantum dots immunofluorescence histochemical detection of EGFR gene mutations in the non-small cell lung cancers using mutation-specific antibodies. Int J Nanomedicine 2014; 9: 5771-5778.
[30] Dawson G. Quantum dots and potential therapy for Krabbe's disease. J Neurosci Res 2016; 94: 1293-1303.